

1 **Overlapping redox zones control arsenic pollution in Pleistocene multi-layer aquifers, the Po**
2 **Plain (Italy)**

3

4 *Marco Rotiroti^{1*}, Tullia Bonomi¹, Elisa Sacchi², John M. McArthur³, Rasmus Jakobsen⁴, Alessandra Sciarra⁵,*
5 *Giuseppe Etiopè⁶, Chiara Zanotti¹, Veronica Nava¹, Letizia Fumagalli¹ and Barbara Leoni¹*

6

7 ¹Department of Earth and Environmental Sciences, University of Milano-Bicocca, Piazza della Scienza 1, 20126 Milan,
8 Italy.

9 ²Department of Earth and Environmental Sciences, University of Pavia, Via Ferrata 1, 27100 Pavia, Italy.

10 ³Department of Earth Sciences, University College London, Gower Street, WC1E 6BT London, United Kingdom.

11 ⁴Geological Survey of Denmark and Greenland, Øster Voldgade 10, 1350 Copenhagen, Denmark.

12 ⁵Istituto Nazionale di Geofisica e Vulcanologia, Sezione Roma 1, Via di Vigna Murata 605, 00143 Rome, Italy.

13 ⁶Istituto Nazionale di Geofisica e Vulcanologia, Sezione Roma 2, Via di Vigna Murata 605, 00143 Rome, Italy.

14 *corresponding author, email: marco.rotiroti@unimib.it, tel: +39 0264482882.

15

16

17 **Abstract**

18 Understanding the factors that control As concentrations in groundwater is vital for supplying safe
19 groundwater in regions with As-polluted aquifers. Despite much research, mainly addressing Holocene aquifers hosting
20 young (<100 yrs) groundwater, the source, transport, and fate of As in Pleistocene aquifers with fossil (>12,000 yrs)
21 groundwaters are not yet fully understood and so are assessed here through an evaluation of the redox properties of the
22 system in a type locality, the Po Plain (Italy).

23 Analyses of redox-sensitive species and major ions on 22 groundwater samples from the Pleistocene arsenic-
24 affected aquifer in the Po Plain shows that groundwater concentrations of As are controlled by the simultaneous
25 operation of several terminal electron accepters. Organic matter, present as peat, is abundant in the aquifer, allowing
26 groundwater to reach a quasi-steady-state of highly reducing conditions close to thermodynamic equilibrium. In this
27 system, simultaneous reduction of Fe-oxide and sulfate results in low concentrations of As (median 7 µg/L) whereas As
28 reaches higher concentrations (median of 82 µg/L) during simultaneous methanogenesis and Fe-reduction. The position
29 of well-screens is an additional controlling factor on groundwater As: short screens that overlap confining aquitards
30 generate higher As concentrations than long screens placed away from them. A conceptual model for groundwater As,

31 applicable worldwide in other Pleistocene aquifers with reducible Fe-oxides and abundant organic matter is proposed:
32 As may have two concentration peaks, the first after prolonged Fe-oxide reduction and until sulfate reduction takes
33 place, the second during simultaneous Fe-reduction and methanogenesis.

34
35 **Keywords:** Groundwater quality, TEAPs, peat, methanogenesis, sulfate, iron.

36

37 **1. Introduction**

38

39 Arsenic pollution of groundwater affects many areas around the world (Ravenscroft et al., 2009). South and
40 South-East Asia are the most As-affected regions worldwide (Fendorf et al., 2010; McArthur, 2019), where over 100
41 million people are being exposed (Ravenscroft et al., 2009), with other regions being less affected. In Europe,
42 groundwater in two large areas is affected by As pollution: a) the Pannonian Basin, covering 325,000 km² (Gyuró,
43 2007) between Hungary, Romania, Serbia, Slovakia and Croatia, with nearly 1 million people exposed to drinking
44 waters with As greater than the WHO standard of 10 µg/L (Rowland et al., 2011); b) the Po Plain of Italy, which covers
45 an area of 46,000 km² and is home to around 20 million inhabitants. In the Po Plain, groundwater for public
46 consumption is treated to keep As <10 µg/L before it is distributed, so As in locally-grown food poses a greater risk
47 than does As in groundwater (Cubadda et al., 2010; Di Giuseppe et al., 2014), owing to the use of As-polluted water for
48 irrigation. Nevertheless, the ability to tap As-free groundwater remains an important target for the managers of any
49 drinking water supply, with a primary aim being to minimize the cost of water purification. Additionally, in the next
50 years, the limit for As of 10 µg/L may be lowered, as it has been in Denmark (5 µg/L; Ersbøll et al., 2018) and may
51 soon be in the Netherlands (1 µg/L; Ahmad et al., 2020). Moreover, following the approach of water safety planning
52 (WSP) recommended by WHO (2011) and implemented by EC (2015) and Italian regulations (D. M. S. 14.06.17,
53 2017), drinking-water managers are required to adopt a preventive approach to mitigate the health risks from As posed
54 to consumers. To this end, the quest for As-free groundwater is key. Although previous studies described the severity of
55 As pollution in the Po Plain, and proposed conceptual models for interpreting As dynamics (Carraro et al., 2015;
56 Cavalca et al., 2019; Giuliano, 1995; Molinari et al., 2013; Rotiroti et al., 2017, 2015; Zuzolo et al., 2020), an in-depth
57 evaluation of the factors controlling the source, transport and fate of As in groundwater is still lacking.

58 Parallels can be drawn between the As-pollution of aquifers beneath the Po Plain and those in South and
59 South-East Asia. In SE Asia, the reductive dissolution of Fe-oxide, driven by organic matter (OM) degradation, is the
60 main mechanism for As release to groundwater (Nickson et al., 1998 et seq.). In SE Asia, As-pollution mostly affects

61 shallow Holocene aquifers (mostly <50 m below ground surface; bgs), whereas deeper Pleistocene aquifers are mostly
62 As-free (Ravenscroft et al., 2009). The difference is attributed to the fact that OM is more abundant in the shallow
63 Holocene aquifers (Ravenscroft et al., 2009; Sutton et al., 2009). The severity of the problem of As-pollution in SE Asia
64 has attracted much research effort focused on Holocene aquifers with young (<100 yrs) groundwaters (Radloff et al.,
65 2017; Richards et al., 2019; Sørensen et al., 2018), whereas Pleistocene aquifers hosting fossil (>12,000 yrs) groundwater, as
66 the case of the Po Plain (Martinelli et al., 2014; Zuppi and Sacchi, 2004), are much less explored.

67 The aim of the present work is to identify the main controls on groundwater As in the deep pre-Holocene
68 aquifers, with the aquifers of the Po Plain being an exemplar, in order to aid prediction of where low-As groundwater
69 can be found in such aquifer, thereby supporting the management of such groundwater resources. To accomplish our
70 aims, new hydrochemical field data, including dissolved CH₄ and H₂, was collected from wells used for irrigation,
71 livestock farming, and public water-supply. The data is used to improve the existing conceptual model for As
72 mobilization in the Po Plain, a model that invokes the reductive dissolution of Fe-oxides driven by the degradation of
73 peat-derived OM.

74

75 **2. Materials and Methods**

76

77 **2.1. Study Area**

78

79 The study area encompasses ~500 km² of the lower Po Plain of North Italy (Fig. S1). This area is the southern
80 portion of a larger area previously studied through 5 field surveys (Sect. 2.2; Rotiroti et al., 2019a, 2019b; Zanotti et al.,
81 2019) that provided a detailed description of the hydrology, hydrogeology and hydrochemistry of the study area: a brief
82 summary is given here. The alluvial sediments of the Po Plain are Pleistocene in age, except for the shallower part (<30-
83 40 m bgs) of the river valleys (Fig. S1) that are filled with Holocene sediments (Marchetti, 2002). Alternating silts/clays
84 and sands (Fig. S1), form a multi-layer stacked aquifer system (Giuliano, 1995; Ori, 1993; Perego et al., 2014). Silt and
85 clay aquitards often contain buried peats (Amorosi et al., 2008; Miola et al., 2006). The aquifers are confined, except
86 where the confining layer thins locally to create semi-confined or unconfined conditions. Groundwater flow in the
87 deeper system (>40 m bgs) is from NW to SE (Fig. S1). In the shallow parts of the system (<40 m bgs), baseflow to
88 local, gaining, rivers imparts strong local variations to the direction of groundwater flow (Rotiroti et al., 2019a).
89 Groundwater recharge is mainly from inflow sourced by upstream areas, as the widespread presence of shallow
90 confining clays and silts prevents or restricts infiltration from surface sources. Locally, however, patchy coarser

91 sediments allow some local recharge by returning irrigation water or infiltration from irrigation channels. In addition, a
92 pumping-induced recharge from rivers or irrigation channels occurs where wells are sited close to surface water bodies
93 (Rotiroti et al., 2019a).

94 Groundwater tracers enabled Rotiroti et al. (2019a) to classify groundwater samples into two groups: a) older
95 groundwaters with little or no local recharge ($Cl/Br < 340$ and $\delta^2H > -60\text{‰}$); and b) younger groundwaters ($Cl/Br > 340$
96 and $\delta^2H < -60\text{‰}$) whose composition approach the values in the Oglio River ($\delta^2H \approx -65\text{‰}$ and Cl/Br between 474 and
97 733). Groundwaters are reducing and of the $Ca-HCO_3$ type, with low Cl content (median concentration of 3.0 mg/L;
98 Rotiroti et al., 2019a).

99

100 **2.2. Groundwater sampling and analysis**

101

102 Groundwater samples were collected in July 2017 from 22 wells (Fig. S1). The wells targeted were those for
103 which complete information was available (well and screen depths, lithology). Most had only one screen, but 2 had two
104 screens and 3 had five screens. Locations were chosen to obtain as regular a sample grid as possible and, where
105 possible, to provide a depth profile, using wells that were close together but had different screened intervals. These
106 wells were sampled 5 times before (October 2015, February, June, September 2016 and March 2017) for the analysis of
107 major ions, trace elements (As, Fe and Mn) and water isotopes; the results were reported in Rotiroti et al. (2019a,
108 2019b). The present study extends the range of parameters measured in those studies, comprising pH, electrical
109 conductivity (EC), oxidation-reduction potential (ORP), dissolved O_2 (DO), water temperature, alkalinity, chloride (Cl),
110 nitrate (NO_3), sulfate (SO_4), ammonium (NH_4), calcium (Ca), magnesium (Mg), sodium (Na), potassium (K), total
111 arsenic (As), As(III), As(V), iron (Fe), manganese (Mn), total phosphorous (P-tot), dissolved organic carbon (DOC),
112 methane (CH_4), dihydrogen (H_2), water isotopes ($\delta^{18}O/\delta^2H$ in H_2O), carbon isotopes ($\delta^{13}C$) in CH_4 (only for 9 samples)
113 and nitrogen isotopes ($\delta^{15}N$) in NH_4 (only for 8 samples collected in September 2016). In addition, measures of the ratio
114 between chloride and bromide (Cl/Br) were available from the previous sampling surveys in June and September 2016
115 (Rotiroti et al., 2019a). Details of sampling methods, field measurements and laboratory analyses are reported in Sup.
116 Info. Sect. S3 together with limits of detection (LOD) and analytical uncertainties (Table S1). Charge-balance error
117 (CBE) was used as a means for evaluating analytical techniques (Fritz, 1994). The average (mean \pm standard deviation)
118 CBE was $0.65 \pm 0.70 \%$ and $0.83 \pm 0.47 \%$ in terms of absolute values, below the recommended threshold of 2% (Fritz,
119 1994). Calculation of speciation and saturation indices (SI's) was done using PHREEQC (Parkhurst and Appelo, 2013)
120 and the wateq4f database (Ball and Nordstrom, 1991). Speciation was computed using pe values derived from field

121 ORP measurements ($E_{\text{Ag}/\text{AgCl}}$). Energetics of terminal electron accepting processes (TEAPs) was assessed by calculating
122 the Gibbs free energy of reaction at system condition using PHREEQC, considering the activities computed during
123 speciation. Reduction half-reactions, with H_2 as electron donor, were considered in this calculation because the H_2 level
124 reflects the internal redox state of many different anaerobic microorganisms, regardless of the main electron donor
125 (Hoehler et al., 2001). Details on stoichiometry are given in Table S2. Since sulfides were not measured in this study,
126 the activity of HS^- was calculated by assuming equilibrium with FeS.

127

128 **3. Results and Discussion**

129

130 **3.1. Peat degradation governs groundwater chemistry**

131

132 Sampled groundwater is reducing and contains <0.2 mg/L of DO and NO_3 . Italian regulatory limits of 10, 200,
133 50 and 500 $\mu\text{g/L}$ for As, Fe, Mn and NH_4 are exceeded, respectively, in 9, 14, 20 and 14 of our 22 well waters (Table
134 S1, Fig. S2). These reducing conditions are generated by the degradation of OM in localized deposits of peat within the
135 clay and silt aquitards. The widespread distribution of peat over the entire depth-range studied (up to 200 m bgs) is
136 confirmed by its recorded presence in numerous lithologs (Bonomi et al., 2014; Rotiroti et al., 2019a) and by other
137 reports of its presence in cores drilled in the lower Po Plain (Carraro et al., 2015; Miola et al., 2006; Rotiroti et al.,
138 2014; Sciarra et al., 2013; Zuppi and Sacchi, 2004). The peats were formed in abandoned meanders and zones of water
139 stagnation generated by river avulsion and subsequently buried by younger alluvium (Miola et al., 2006). Microbial
140 metabolism of sedimentary OM generates organic molecules, ammonium, and phosphate, which are released to
141 groundwater along with Br (Gerritse and George, 1988). Although typically treated as conservative in groundwater, the
142 Cl/Br of unpolluted groundwater may decline as OM degradation releases more Br than Cl. Ammonium can have a
143 conservative behavior under strong reducing conditions, although it can be removed from groundwater by cation
144 exchange: a consequence of ion-exchange is to lessen the concentration even where a steady supply of NH_4 is available
145 *via* organic degradation. Our recorded concentrations of NH_4 are therefore not an indication of total OM mineralization.
146 Nevertheless, increasing DOC and NH_4 , and decreasing Cl/Br values, trace the progression of OM degradation (Böhlke
147 et al., 2006; Desbarats et al., 2014). The strong positive correlation of DOC with NH_4 and P-tot (Pearson correlation
148 coefficient r of 0.98 and 0.95 with p-values of $6.5e^{-16}$ and $4.5e^{-13}$, respectively; Table S3) and the negative correlation
149 of Cl/Br with DOC (r of -0.74 with p-value of $3.8e^{-5}$; Table S3), and thus with NH_4 and P-tot, found in our data (Fig. 1)
150 indicate that the studied system is experiencing OM degradation with an accumulation of by-products.

151 Based on predominant TEAPs, the sampled groundwaters may be grouped into three classes (Fig. 1); these are:
152 1) Fe-oxide reduction and early-stage sulfate reduction for samples with $\text{SO}_4 > 10$ mg/L; 2) Fe-oxide reduction and
153 advanced-stage sulfate reduction with $\text{SO}_4 < 10$ mg/L and $\text{CH}_4 < 0.5$ mg/L; 3) Fe-oxide reduction and methanogenesis
154 with $\text{SO}_4 < 1.5$ mg/L and $\text{CH}_4 > 0.5$ mg/L. The expected succession through the classes, the clean transition between
155 them seen in our data, and the accompanying increasing DOC and NH_4 and decreasing Cl/Br, all confirm that there is a
156 progressing degradation of OM within the system. This evidence of degradation, together with the fact that this redox
157 classification was based on Fe, SO_4 and CH_4 rather than on DOC, NH_4 and Cl/Br, validates our classification. Fe-oxide
158 reduction is considered to occur in all these three classes due to the presence of dissolved Fe (median concentration for
159 all samples of 274 $\mu\text{g/L}$) and the considerations discussed in depth in Sect. 3.2. Concerning P-tot, its strong positive
160 correlation with DOC is probably a result of the release of P from degrading OM. Additionally, the reductive
161 dissolution of Fe-oxides, on which P is likely adsorbed (Ravenscroft et al., 2001), gives an extra input of P-tot to
162 groundwater. Since Fe-oxides reduction proceeds together with OM degradation, the contribution from the two sources
163 cannot be separated.

164 Microbial degradation of peat is also the likely source of dissolved CH_4 in groundwater, as suggested by the
165 positive correlation between DOC and CH_4 (r of 0.90 with p-value of $1.9e^{-9}$; Table S3; data plotted in Fig. 1) and
166 $\delta^{13}\text{C}_{\text{CH}_4}$ values (from -75.2 to -62.4%) that fall within the range of microbial methane (Mattavelli and Novelli, 1988;
167 Milkov and Etiope, 2018). More specifically, the $\delta^{13}\text{C}$ values in four wells (LL50 and LR59-61) are $< -70\%$ (Table S1)
168 indicating a source *via* CO_2 reduction (Milkov and Etiope, 2018; Whiticar, 1999), as in other aquifers worldwide
169 (Aravena et al., 1995; Coleman et al., 1988; Hansen et al., 2001; Postma et al., 2012). In another five wells, $\delta^{13}\text{C}$
170 $> -70\%$, indicating a source *via* acetate fermentation. Furthermore, values of $\delta^{15}\text{N}_{\text{NH}_4}$ ranging from 1.3 to 16.0‰
171 confirm that NH_4 is the product of local degradation of peat (see Sup. Info. Sect. S4). Finally, some thrust systems,
172 which could facilitate the seepage of deep gas, are located within or close to the study area (Lindquist, 1999; Maesano
173 and D'Ambrogi, 2016; Mattavelli et al., 1983; Rossi et al., 2015). Whilst we cannot exclude the possibility that such
174 seepage contributes to our measured concentrations of CH_4 , the good correlation between CH_4 and DOC suggests that
175 such an influence is not present.

176 The degradation of OM is a strong influence on alkalinity and EC, and generates a positive correlation between
177 DOC and, for example, Na and Ca (see Sup. Info. Sect. S5 for further details). The strong correlation of alkalinity with
178 DOC (Fig. 1) and NH_4 (r of 0.84 and 0.85 with p-values of $3.6e^{-7}$ and $1.5e^{-7}$, respectively; Table S3) is the likely effect
179 of dissolved inorganic carbon (DIC) production due to the mineralization of sedimentary OM, both as direct oxidation
180 of organic to inorganic carbon and dissolution of carbonate minerals in response to the increase of acidity generated by

181 the fermentation of OM (producing CO₂ and organic acids) during its degradation (Buckau et al., 2000). Speciation and
182 calculation of SI's revealed that the role of buffering the increase in acidity is here likely played by the dissolution of
183 rhodochrosite (MnCO₃), for which the groundwater was found to be near equilibrium, whereas a strong supersaturation
184 was seen for calcite (CaCO₃), dolomite (MgCa(CO₃)₂) and siderite (FeCO₃; see Sup. Info. Sect. S6 for further details).
185 The strong correlation of EC with DOC (Fig. 1) and NH₄ (*r* of 0.81 and 0.83 with *p*-values of 1.9e⁻⁶ and 4.3e⁻⁷,
186 respectively; Table S3), that are all products or effects of OM degradation, indicates that groundwater salinity is mainly
187 due to OM degradation. The low Cl concentrations in our groundwaters confirm that anthropogenic influences are
188 insignificant in all but three wells (LL39, LL41, LR58) that contain between 19 and 34 mg/L of SO₄ and have Cl/Br
189 >400. These three contain a vestigial anthropogenic influence inherited from upstream recharge areas. Higher δ¹⁸O and
190 δ²H values with increasing EC indicate that younger, human-impacted, recharge from the surface, having more depleted
191 isotope values (Rotiroti et al., 2019a), does not contribute significantly to the EC. This confirms that the main source of
192 OM is buried peat, indicating that a possible infiltration of OM from the surface, either of anthropogenic (e.g. sewage,
193 manure) or natural (e.g. riverine) origin, is unlikely or minor.

194

195 **3.2. Different TEAPs occur simultaneously: overlapping redox zones**

196

197 Traditionally, the sequence of TEAPs accompanying OM oxidation follow a hierarchy of decreasing Gibbs
198 free energy (Champ et al., 1979; Lovley and Goodwin, 1988; McMahon and Chapelle, 2008). This linear succession of
199 redox reactions and zones implies that competitive exclusion exists within bacteria communities that mediate successive
200 redox zones (Chapelle and Lovley, 1992). It is clear from our data, however, that for the least energetically favored
201 TEAPs, the conventional fixed hierarchical sequence does not apply in groundwaters at circumneutral pH. Instead, Fe-
202 oxide reduction, sulfate reduction and methanogenesis can proceed either in a different order or simultaneously, as
203 suggested for groundwater elsewhere (Bethke et al., 2011; Postma and Jakobsen, 1996). The reasons for this different
204 order are several. Firstly, Fe-oxide reduction is pH-dependent and, at circumneutral pH, the reduction of more stable Fe-
205 oxides (e.g. magnetite, goethite) is energetically unfavorable (lower release of Gibbs free energy) with respect to
206 methanogenesis and sulfate reduction (Bethke et al., 2011). Secondly, considering usable, rather than available, energy
207 (the difference between the available energy and that maintained by bacteria to sustain their life functions; Jin and
208 Bethke, 2009, 2003), Fe-oxide reduction, sulfate reduction and methanogenesis provide approximately the same
209 amounts of energy at near neutral pH in groundwater (Bethke et al., 2011). Thus, energetics cannot establish a fixed
210 order for the progression of late stage redox reactions. Thirdly, microbial ecology suggests that mutualistic, rather than

211 competitive, relationships between bacteria may mediate the use of TEAPs, so the simultaneous use of two TEAPs
212 might be favored; for example, by the removal by precipitation of their by-products, as postulated for the simultaneous
213 operation of Fe-oxide reduction and sulfate reduction aided by precipitation of iron sulfide (Bethke et al., 2011; Postma
214 and Jakobsen, 1996), and simultaneous Fe-oxide reduction and methanogenesis with precipitation of siderite (Jakobsen
215 and Cold, 2007).

216 Although microbial ecology and kinetic limitations play a role, together with microbial microenvironments
217 (Murphy et al., 1992), in which favorable conditions for specific TEAPs can develop locally on a micro scale (e.g. the
218 increase in acidity in a biofilm surrounding a fragment of fermenting OM can favor local goethite reduction; Bethke et
219 al., 2011) an aquifer system with a high supply of OM developing strong reducing conditions (where Fe-oxide
220 reduction, sulfate reduction and methanogenesis can take place) can be well-described, on the whole, by equilibrium
221 thermodynamics (Bethke et al., 2011), according to the partial equilibrium approach (Postma and Jakobsen, 1996). This
222 considers the OM degradation as a two-steps process (Lovely, 1987): 1) the hydrolyzation and fermentation of OM with
223 the production of simpler compounds as formic acid, acetic acid, H₂ and CO₂; this is the rate-determining step; 2) the
224 consumption of the fermentative products by different TEAPs; this step is assumed to approach equilibrium. However,
225 full equilibrium is not obtained as a small amount of energy is used for growth by the microorganisms mediating the
226 processes. The partial equilibrium approach is applicable for Mn-oxide, Fe-oxide and sulfate reduction and
227 methanogenesis, but it is not adequate for DO reduction and denitrification since they involve a direct OM
228 metabolization by bacteria (Appelo and Postma, 2005).

229 Our sampled groundwaters are in redox states where the electron acceptors for DO reduction, denitrification
230 and Mn-oxide reduction have been exhausted (DO and NO₃ <0.2 mg/L and mean Mn = 110 µg/L), so Fe-oxide
231 reduction, sulfate reduction and methanogenesis either occur successively as the predominant TEAP (in the classical
232 view) or occur simultaneously. In our system, the simultaneous occurrence of Fe-oxide and sulfate reduction, together
233 with the precipitation of their products as iron sulfides, is supported by the plot of Fig. 2a, showing that many samples
234 are aligned along a slope similar to the equilibrium lines of simultaneous Fe-oxide reduction, sulfate reduction and FeS
235 precipitation (the stoichiometry and the equilibrium equation are given in Table S4). Moreover, many groundwaters fit
236 a modelled equilibrium involving a hypothetical Fe-oxide (solubility product for which logK is 0.78; Rotiroti et al.,
237 2015) that is in the range of stability of goethite and lepidocrocite (Cornell and Schwertmann, 2003). This phase may be
238 considered as a theoretical, moderately stable, Fe-oxide, representing the average of a mixture of low and high stability
239 oxides likely present in the aquifer, for which the overall system approaches a thermodynamic equilibrium. The fact that
240 the composition of three groundwaters that are classified as Fe-oxide reduction and methanogenesis (wells LR59-61)

241 align with this equilibrium line could indicate that sulfate reduction may still be ongoing, likely at slow rates, even
242 where methanogenesis is predominant. Alternatively, the simultaneous operation of Fe-oxide reduction, sulfate
243 reduction and methanogenesis could be apparent, being, actually, the effect of mixing along well screens of
244 groundwaters coming from different zones and having different conditions.

245 Notwithstanding the above, three other groundwaters that are classed as Fe-oxide reduction and
246 methanogenesis (wells LL47, LL50 and OV77) depart more from equilibrium, likely indicating that, in these
247 groundwaters, sulfate reduction is not occurring, but that methanogenesis occurs simultaneously with Fe-oxide
248 reduction. This interpretation is supported by a) the proximity of these three samples (wells LL47, LL50 and OV77) to
249 the equilibrium line of simultaneous Fe-oxide reduction and methanogenesis (Fig. 2a; see Table S4 for stoichiometry
250 and equilibrium equation) and b) the positive correlation of Fe with DOC and CH₄ (Fig. S3) for groundwaters with Fe-
251 oxide reduction and methanogenesis. Fe-oxide reduction and methanogenesis were previously reported to occur
252 concomitantly near equilibrium in reducing groundwaters worldwide (Jakobsen and Cold, 2007; Postma et al., 2007;
253 Zhou et al., 2014) and simulated through modelling (Jakobsen, 2007; Rotiroti et al., 2018). Their simultaneous
254 occurrence could be the result of a mutualistic relationship between Fe-reducing bacteria and methanogens aided by the
255 precipitation of siderite (Jakobsen and Cold, 2007). However, siderite precipitation often occurs far from equilibrium
256 (i.e. at supersaturation; Postma, 1982) due to a kinetic inhibition exerted by OM and PO₄ (Berner et al., 1978). Kinetic
257 inhibition seems confirmed in our system by the supersaturation seen for siderite and the correlation between its SI and
258 DOC (Sup. Info. Sect. S6).

259 Additional evidence of the presence of overlapping redox zone in our groundwaters can be obtained from a
260 further consideration of energetics. Fig. 2b shows computed values of Gibbs free energy of reaction at our system
261 conditions (ΔG_r) for Fe-oxide reduction (considering the various oxides at different stabilities listed in Table S2),
262 sulfate reduction and methanogenesis, compared to a range of threshold energy values (ΔG_{min} ; representing the energy
263 level maintained by the microbes) taken from literature (Hoehler, 2004; Jakobsen and Cold, 2007; Rotiroti et al., 2018),
264 so that an estimation of the usable energy ($\Delta G_r - \Delta G_{min}$) can be given. The usable energy for all the three TEAPs
265 (considering the hypothetical medium-stable oxide for Fe-reduction) results in the order of a few kJ/mol per H₂ (Fig.
266 2b), confirming the findings by Bethke et al. (2011) of roughly equivalent amounts. Fe-oxide reduction is more
267 favorable ($\Delta G_r < \Delta G_{min}$) for relatively unstable oxides, such as lepidocrocite and ferrihydrite (not shown), and
268 unfavorable ($\Delta G_r > \Delta G_{min}$) for relatively stable oxide, such as goethite and hematite (not shown). The reduction of the
269 hypothetical middle-stability oxide (representing average system-conditions), for which most of the samples align in the
270 plot of Fig. 2a, has an available energy, for all samples, in the range of the threshold energy ($\Delta G_r \approx \Delta G_{min}$), giving a

271 usable energy close to zero. An energy close to zero thus confirms that Fe-oxide reduction may occur close to a
272 thermodynamic equilibrium in all the three classes of samples identified here. A similar condition (i.e. $\Delta G_r \approx \Delta G_{\min}$) is
273 found for sulfate reduction in samples classified as ‘Fe-oxide reduction and advanced-stage sulfate reduction’ and for
274 methanogenesis in samples classified as ‘Fe-oxide reduction and methanogenesis’. The usable energy close to zero for
275 a) Fe-oxides reduction and b) sulfate reduction or methanogenesis confirms the presence in our samples of a “partial”
276 equilibrium state in which simultaneous Fe-oxide reduction/sulfate reduction or Fe-oxide reduction/methanogenesis can
277 occur, respectively.

278 Finally, some considerations must be given to Mn-oxide reduction. The assertion made above that Mn-oxide
279 reduction is complete in our groundwaters is supported by Fig. S4, in which samples plot far from, and with a different
280 slope to, the equilibrium line for Mn-oxide reduction. This departure from equilibrium precludes equilibrium with other
281 TEAPs. We propose that Mn-oxide reduction occurred upflow in the aquifer in earlier stages of OM degradation and so
282 has not been captured by our samples as the product of Mn-reduction. Rather, we propose that dissolved Mn in our
283 groundwaters, produced upflow, is now controlled by the dissolution/precipitation equilibrium of rhodochrosite. This
284 equilibrium, together with the likely role played by rhodochrosite in buffering acidity, as discussed in Sect. 3.1, implies
285 that high Mn concentrations are maintained by rhodochrosite dissolution. Such a proposal agrees with the fact that
286 selective sequential extractions of aquifer sediments from the Po Plain showed that Mn is mostly present in the
287 sediment as carbonate (Molinari et al., 2014).

288

289 **3.3. What controls groundwater As?**

290

291 The positive correlation of As with DOC, NH_4 and P-tot (r of 0.87, 0.89 and 0.90 with p-values of $3.6e^{-8}$,
292 $7.7e^{-9}$ and $3.1e^{-9}$, respectively; Table S3) and its negative correlation with Cl/Br (r of -0.65 with p-value of $6.1e^{-4}$;
293 Table S3; data plotted in Fig. 3) confirm that the degradation of peat is the driver of As release to groundwater in the Po
294 Plain. Although As and Fe concentrations are frequently reported to have a poor correlation (see Ravenscroft et al.,
295 2009 for reviews) because Fe is not conservative in solution, they show a covariation in our system, albeit weak, for
296 groundwaters under methanogenesis (Fig. 3), confirming that Fe-oxide is the source of As release. Furthermore, the fact
297 that dissolved As is present predominantly as As(III) in our groundwaters (Table S1) corroborates our view that
298 reductive dissolution of Fe-oxide, driven by peat degradation, causes As-pollution of our groundwaters. However, the
299 strong correlation of As with the products of OM degradation (Fig. 3), such as DOC, NH_4 and CH_4 (r of 0.97 with p-
300 value of $8.9e^{-15}$; Table S3), can also indicate that As can also be released directly by peat degradation. During its

301 formation and evolution, peat can sequester As by forming covalent bonds between dissolved As and its sulfur groups
302 (Anawar et al., 2003; Eberle et al., 2020; Langner et al., 2012;), so the prolonged degradation of peat can be a direct
303 source of As to groundwater. The content of As on OM in solid aquitard samples from the Po Plain was reported by
304 Molinari et al. (2015) to be between 13.1 and 26.0% of total As in the solid matrix, the larger fraction (41 to 84%) being
305 found in Fe and Mn oxyhydroxides and crystalline oxides, so aquitard OM represents a relevant potential source of As
306 to groundwater in this system.

307 The mutual exclusion of As and SO_4 (Fig. 3) indicates that sulfate reduction, occurring together with Fe-oxide
308 reduction, leads to As sequestration *via* co-precipitation in FeS, formed by the products of these two reduction
309 reactions, and/or via direct precipitation of As-sulfides (O'Day et al., 2004). The strong positive correlation between As
310 and CH_4 (Fig. 3) is interpreted to be the result of the cessation of As sequestration by iron sulfides produced during
311 sulfate reduction. Methanogenesis takes place after sulfate reduction is completed, as testified by the mutual exclusion
312 between CH_4 and SO_4 (Fig. S5), so the appearance of CH_4 marks the end of the As sequestration into precipitating
313 sulfides. Therefore, during methanogenesis and Fe-reduction, As is released (from both reductive dissolution and peat
314 degradation) with no or little attenuation processes, reaching the highest concentrations found in the groundwater.

315 The conclusion that As is high in groundwater during methanogenesis and Fe-reduction is confirmed by the
316 interpretation of H_2 data, which are plotted against DOC and As in Fig. S6. Concentrations of As are low in
317 groundwaters when simultaneous reduction of both Fe-oxide and sulfate occurs and also H_2 concentrations are between
318 1 and 4 nM, values that indicate active sulfate reduction (Chapelle et al., 1995). Concentrations of As are higher in
319 groundwaters where both Fe-oxide reduction and methanogenesis occur together and concentrations of H_2 are between
320 2.7 and 4.7 nM. Although H_2 concentrations in both cases are below 5 nM, the minimum threshold proposed for
321 methanogenesis by Chapelle et al. (1995), they are in the range 2–5 nM reported by Kirk et al. (2004) for groundwaters
322 in which maximal concentrations of As occurred where both Fe-oxide reduction and methanogenesis was occurring
323 simultaneously. Hansen et al. (2001) and Jakobsen and Cold (2007) also report the occurrence of methanogenesis
324 together with Fe-oxide reduction when concentrations of H_2 are below 5 nM.

325 Concentrations of As in well water also may depend on the proximity of the screened interval(s) to organic-
326 rich aquitards from which OM degradation by-products may be supplied by aquitard diffusion (McMahon and Chapelle,
327 1991). Wells screened proximally to aquitards have higher concentrations of As than do wells screened distally
328 (Erickson and Barnes, 2005; Meliker et al., 2008). Longer screens, having a higher proportion of distal screen, also have
329 lower As concentrations than do short screens where all the screen may be close to an aquitard (Erickson and Barnes,
330 2005; Meliker et al., 2008). For our wells, the linear or near-linear relations shown in Fig. 1 and 3, for samples

331 characterized by Fe-oxide reduction and methanogenesis, may indicate that the position of the screens with respect to
332 aquitards is also affecting As concentrations in our wells. The highest As value (184 µg/L) was measured in well OV77
333 which has 2 m (out of 9.5 m) of screen juxtaposed to a clay interval, whereas the lowest As for samples characterized
334 by Fe-oxide reduction and methanogenesis (40 µg/L) was found in well LR60 in which no part of the 15 m screen was
335 withing 1.5 m of a clay aquitard (we discount well LL47 with 31 µg/L of As because we have no information on
336 lithology or screen interval). In well LR59, which has 104 µg/L of As in its water, an intermediate condition is found: a
337 screen 4 m long is placed adjacent to a confining clay. These observations support the hypothesis that the position of
338 well screens can influence As concentrations in abstracted groundwaters.

339

340 **3.4. The “two-peaks” conceptual model for groundwater As**

341

342 Fig. 4 schematizes, for the aquifer systems of the Po Plain, how the concentrations of As and other redox
343 species evolve during ongoing degradation of peat: the figure is based both on our data and the work of others (e.g.
344 Appelo and Postma, 2005; Berner, 1981; Kirk et al., 2004; McArthur et al., 2004; Rotiroti et al., 2014; Sracek et al.,
345 2018). In a system dominated by piston flow (i.e. with no mixing of groundwaters), the accumulated effect of the peat
346 degradation is a function of time and so related to groundwater age; composition reflects an integration of all upstream
347 reactions with those occurring in the present. At early stages of Fe-oxide reduction, and during Mn-oxide reduction,
348 groundwater As is low due to its re-sorption onto residual oxides (Welch et al. 2000; McArthur et al., 2004). With the
349 progression of Fe-oxide reduction, empty sorption sites on residual Fe-oxides decrease and dissolved As increases
350 generating a first peak in As concentration. With the occurrence of sulfate reduction, dissolved As is attenuated by co-
351 precipitation in FeS and/or precipitation in As-sulfides, such as realgar or orpiment (Carraro et al., 2015). The degree of
352 attenuation depends on the amount of sulfate present and the proportion that is reduced. The degree of attenuation also
353 depends on the degree of overlap between Fe-oxide reduction and sulfate reduction, which in turn is governed by the
354 stability of Fe-oxides, pH and microbial ecology. Once sulfate reduction is complete, and methanogenesis occurs
355 together with Fe-oxide reduction, dissolved As increases again. For this second peak in As concentration there will be
356 little attenuation because most reactive Fe-oxides with large surface areas (i.e. sorption sites) have been reduced. The
357 second peak concentration may exceed that of the first peak because of the possible derivation of some As directly from
358 the OM itself. Dissolved As might increase until OM is completely mineralized or the system runs out of reducible Fe-
359 oxide. After this point, dissolved As may decrease due to no new release and the attenuation of already released As.
360 This could explain the decrease of As that is frequently found in the Po Plain aquifers at depth around and below 200 m

361 bgs (Carraro et al., 2015; Rotiroti et al., 2014), where groundwaters can have ages up to ~50 kyrs (Martinelli et al.,
362 2014; Zuppi and Sacchi, 2004). The attenuation must be assisted by a) dispersion, b) diffusion, c) flushing, albeit
363 probably weak since groundwater at these depths have a sluggish circulation (hydraulic gradient around 0.1%; Rotiroti
364 et al., 2019a) and d) adsorption onto siderite (Burnol and Charlet, 2010; Kocar et al., 2014) or other minerals. The last
365 could be facilitated after the system has experienced prolonged and simultaneous Fe-oxide reduction and
366 methanogenesis, a condition that may be favored by siderite precipitation (Sect. 3.2).

367 This conceptual model is based on the assumption of a widespread presence of reducible Fe-oxides and buried
368 peat in the system, the latter ensures a large stock of OM, providing a constant OM input to the aquifer, a condition that
369 seems to be valid in the study area and in the entire lower Po Plain (Carraro et al., 2015; Rotiroti et al., 2015; Sciarra et
370 al., 2013), although our DOC levels did not reach high levels, as reported in other OM-rich aquifers worldwide (Buckau
371 et al., 2000).

372 The application of our conceptual model helps to interpret the variability of As in space and over depth in the
373 study area. There is no relation between depth and redox states (Fig. S7), and thus, according to the conceptual model,
374 between depth and As. For instance, methanogenesis takes place both at shallower and deeper depths, therefore high As
375 values can be found both in shallow (e.g. well LR59) and deep (e.g. well OV77) groundwaters. Based on our data
376 analyses, this means that groundwaters at the same depth can have different ages. Groundwater ages are related to
377 geographical location, determining the length of groundwater flowpaths: wells located in the north-western part of the
378 study area, upstream with respect to groundwater flow (Fig. S1), have shorter flowpaths, younger groundwater ages and
379 higher redox states, whereas those located downstream in the south-eastern zone (Fig. S1), have longer flowpath, older
380 ages and lower redox states. In addition to this, wells with a component of younger recharge, due to pumping-induced
381 recharge from nearby rivers or irrigation channels (Rotiroti et al., 2019a), have an average groundwater age that is
382 younger than ages for water from more distal wells (e.g. wells LL51 and LR58; Fig. S1), so the redox states are higher
383 and As accordingly lower. In other words, younger recharge from the surface, probably containing higher SO₄ (and
384 NO₃), favors sulfate reduction (or denitrification, which is energetically favorable compared to Fe-oxide reduction)
385 suppressing As release.

386

387 **3.5. Worldwide implications**

388

389 A brief comparison of main factors controlling As pollution in South and South-East Asia with those in the Po
390 Plain is discussed below. Concerning the Holocene aquifers in SE Asia, concentrations of dissolved As decline as

391 sediment age increases and OM reactivity decreases (Postma et al., 2012; Stuckey et al., 2016). An additional constrain
392 on As concentration is groundwater residence time (Sø et al., 2018), which determines the time available for
393 sediment/groundwater interaction, the number of pore volumes flushed through the aquifer system, and controls the
394 removal of dissolved and desorbed reaction products. In Vietnam, the deeper Pleistocene aquifers contain >10 µg/L As
395 only where extensive pumping has localized drawdown of As and/or OM from shallow, Holocene, aquifers (Winkel et
396 al., 2011). In the Bengal Basin, As polluted groundwaters in the deep Pleistocene aquifer are found almost invariably in
397 the absence of a palaeosol aquiclude that separates Holocene and Pleistocene aquifers across significant parts of the
398 basin (McArthur et al., 2008, 2016), facilitating the downward of OM driving As release (McArthur, 2019) or recharge
399 of As-rich water from the Holocene as a result of groundwater pumping, although two instances of As-pollution by
400 aquitard diffusion has been reported (Planer-Friedrich et al., 2012; Mihajlov et al., 2020).

401 Unlike South and South-East Asia where the availability of OM is limited in deeper Pleistocene aquifers
402 (Ravenscroft et al., 2009; Sutton et al., 2009), the OM is not limited over depth in the Po Plain where peat deposits are
403 found at depths up to ~250 m bgs (Rotiroti et al., 2014). This is a substantial difference between the two aquifer systems
404 implying that different key factors are controlling As pollution. For instance, younger sediment age and higher OM
405 reactivity seem to have no role in determining As pollution in the Po Plain aquifer system, since here severe As
406 pollution can be found also in groundwater hosted by older sediments, e.g. well LR61 with 177 µg/L of As taps two
407 sandy layers from 97 to 103 and from 151 to 153 m bgs that have an age ranging between 0.45 and 0.63 Myrs (Maesano
408 and D'Ambrogio, 2016). The finding for the study area that As pollution is more severe where methanogenesis takes
409 place once sulfate reduction is complete has been reported to occur in other aquifers that contain abundant OM, such as
410 the Hetao Plain of China (Wang et al., 2015), the Pannonian Basin between Hungary and Romania (Rowland et al.,
411 2011) and the Mahomet and Glasford aquifers in Illinois, USA (Kelly et al., 2005; Kirk et al., 2004). Therefore, it
412 appears that the conceptual model discussed in the present study can be applied to As polluted aquifers worldwide that
413 contain abundant OM, together with reducible Fe-oxides, that allow groundwater to reach a quasi-steady-state of highly
414 reducing conditions (close to thermodynamic equilibrium) and so generate overlapping redox zones.

415

416 **4. Conclusions**

417

418 The key factors controlling As pollution in groundwater of the Po Plain, Italy, may apply in other Pleistocene
419 aquifers with fossil groundwaters worldwide, they are summarized below:

- 420
- the abundant organic matter, present as peat, coupled to much reducible Fe-oxide, allows groundwater
421 to reach a quasi-steady-state of highly reducing conditions close to thermodynamic equilibrium,
422 enabling the simultaneous operation of different TEAPs in overlapping redox zones;
 - the main factor controlling the concentration of As in groundwater is the accumulated effect of peat
423 degradation as reflected in groundwater age: simultaneous Fe-oxide reduction and methanogenesis
424 leads to high-As groundwaters, whereas simultaneous Fe-oxide and sulfate reduction leads to low-As
425 groundwaters;
 - the proximity of well-screens to organic-rich aquicludes influences As concentrations in abstracted
426 groundwaters: As concentrations are higher where screens are proximal to organic-rich aquicludes and
427 lower when the screens are distal to such units;
 - a “two-peaks” conceptual model for groundwater As can be implemented for the Po Plain and other
428 Pleistocene aquifers with similar sediment composition worldwide: a first peak in As concentration
429 occurs after prolonged Fe-oxide reduction and is diminished by sulfate reduction. The peak of As
430 concentration depends on the degree of overlap between Fe-oxide reduction and sulfate reduction; the
431 greater the overlap, the lower the As peak may be, subject to initial SO₄ concentrations, the stability of
432 Fe-oxides, pH and microbial ecology. A second peak of As is reached during simultaneous Fe-
433 reduction and methanogenesis, during which process As is released with no or little attenuation, so it
434 can reach the highest concentrations.
435
436
437

438

439 **Funding**

440

441 This work was supported by Fondazione Cariplo [grant number 2014-1282] and through the scientific collaboration no.
442 2018-CONV25-0024 between University of Milano-Bicocca and INGV.

443

444 **Acknowledgements**

445

446 We thank Acque Bresciane, Padania Acque, A2A Ciclo Idrico and all private owners for letting us to sample their
447 wells. We are grateful to Gennaro A. Stefania, Sara Taviani and Martina Patelli of University of Milano-Bicocca for
448 field work, Valentina Soler and Maria Tringali of University of Milano-Bicocca for major ions and trace elements

449 analyses, Gabriele Tartari of CNR-IRSA (Verbania, Italy) for DOC analysis and Vittorio Barella and Enrico Allais of
450 ISO4 (Torino, Italy) for water and ammonium isotope analyses.

451

452 **Appendix A: Supporting Information**

453

454 Supporting information to this article can be found online at ...

455

456 **References**

457

458 Ahmad, A., van der Wens, P., Baken, K., de Waal, L., Bhattacharya, P., Stuyfzand, P., 2020. Arsenic reduction to
459 $<1 \mu\text{g/L}$ in Dutch drinking water. *Environ. Int.* 134, 105253. <https://doi.org/10.1016/j.envint.2019.105253>

460 Amorosi, A., Pavesi, M., Ricci Lucchi, M., Sarti, G., Piccin, A., 2008. Climatic signature of cyclic fluvial architecture
461 from the Quaternary of the central Po Plain, Italy. *Sediment. Geol.* 209, 58–68.
462 <https://doi.org/10.1016/J.SEDGEO.2008.06.010>

463 Anawar, H.M., Akai, J., Komaki, K., Terao, H., Yoshioka, T., Ishizuka, T., Safiullah, S., Kato, K., 2003. Geochemical
464 occurrence of arsenic in groundwater of Bangladesh: sources and mobilization processes. *J. Geochem. Explor.* 77,
465 109–131. [https://doi.org/10.1016/S0375-6742\(02\)00273-X](https://doi.org/10.1016/S0375-6742(02)00273-X)

466 Appelo, C.A.J., Postma, D., 2005. *Geochemistry, Groundwater and Pollution*, second. ed. Balkema Publishers, Leiden.

467 Aravena, R., Wassenaar, L.I., Barker, J.F., 1995. Distribution and isotopic characterization of methane in a confined
468 aquifer in southern Ontario, Canada. *J. Hydrol.* 173, 51–70. [https://doi.org/10.1016/0022-1694\(95\)02721-Z](https://doi.org/10.1016/0022-1694(95)02721-Z)

469 Ball, J.W., Nordstrom, D.K., 1991. User's manual for WATEQ4F, with revised thermodynamic data base and text cases
470 for calculating speciation of major, trace, and redox elements in natural waters. U.S. Geological Survey Open-File
471 Report 91–183. <https://doi.org/10.3133/ofr91183>

472 Berner, R.A., 1981. A new geochemical classification of sedimentary environments. *J. Sediment. Res.* 51, 359–365.
473 <https://doi.org/10.1306/212F7C7F-2B24-11D7-8648000102C1865D>

474 Berner, R.A., Westrich, J.T., Graber, R., Smith, J., Martens, C.S., 1978. Inhibition of aragonite precipitation from
475 supersaturated seawater; a laboratory and field study. *Am. J. Sci.* 278, 816–837.
476 <https://doi.org/10.2475/ajs.278.6.816>

477 Bethke, C.M., Sanford, R.A., Kirk, M.F., Jin, Q., Flynn, T.M., 2011. The thermodynamic ladder in geomicrobiology.
478 *Am. J. Sci.* 311, 183–210. <https://doi.org/10.2475/03.2011.01>

479 Böhlke, J.K., Smith, R.L., Miller, D.N., 2006. Ammonium transport and reaction in contaminated groundwater:
480 Application of isotope tracers and isotope fractionation studies. *Water Resour. Res.* 42, W05411.
481 <https://doi.org/10.1029/2005WR004349>

482 Bonomi, T., Fumagalli, L., Rotiroti, M., Bellani, A., Cavallin, A., 2014. The hydrogeological well database
483 TANGRAM©: a tool for data processing to support groundwater assessment. *Acq. Sott. Ital. J. Groundw.* 3, 35–
484 45. <https://doi.org/10.7343/as-072-14-0098>

485 Buckau, G., Artinger, R., Geyer, S., Wolf, M., Fritz, P., Kim, J.I., 2000. Groundwater in-situ generation of aquatic
486 humic and fulvic acids and the mineralization of sedimentary organic carbon. *Appl. Geochem.* 15, 819–832.
487 [https://doi.org/10.1016/S0883-2927\(99\)00078-5](https://doi.org/10.1016/S0883-2927(99)00078-5)

488 Burnol, A., Charlet, L., 2010. Fe(II)–Fe(III)-Bearing Phases As a Mineralogical Control on the Heterogeneity of
489 Arsenic in Southeast Asian Groundwater. *Environ. Sci. Technol.* 44, 7541–7547.
490 <https://doi.org/10.1021/es100280h>

491 Carraro, A., Fabbri, P., Giaretta, A., Peruzzo, L., Tateo, F., Tellini, F., 2015. Effects of redox conditions on the control
492 of arsenic mobility in shallow alluvial aquifers on the Venetian Plain (Italy). *Sci. Total Environ.* 532, 581–594.
493 <https://doi.org/10.1016/J.SCITOTENV.2015.06.003>

494 Cavalca, L., Zecchin, S., Zaccheo, P., Abbas, B., Rotiroti, M., Bonomi, T., Muyzer, G., 2019. Exploring Biodiversity
495 and Arsenic Metabolism of Microbiota Inhabiting Arsenic-Rich Groundwaters in Northern Italy. *Front.*
496 *Microbiol.* 10, 1480. <https://doi.org/10.3389/fmicb.2019.01480>

497 Champ, D.R., Gulens, J., Jackson, R.E., 1979. Oxidation–reduction sequences in ground water flow systems. *Can. J.*
498 *Earth Sci.* 16, 12–23. <https://doi.org/10.1139/e79-002>

499 Chapelle, F.H., Lovley, D.R., 1992. Competitive Exclusion of Sulfate Reduction by Fe(III)-Reducing Bacteria: A
500 Mechanism for Producing Discrete Zones of High-Iron Ground Water. *Groundwater* 30, 29–36.
501 <https://doi.org/10.1111/j.1745-6584.1992.tb00808.x>

502 Chapelle, F.H., McMahon, P.B., Dubrovsky, N.M., Fujii, R.F., Oaksford, E.T., Vroblesky, D.A., 1995. Deducing the
503 Distribution of Terminal Electron-Accepting Processes in Hydrologically Diverse Groundwater Systems. *Water*
504 *Resour. Res.* 31, 359–371. <https://doi.org/10.1029/94WR02525>

505 Coleman, D.D., Liu, C.-L., Riley, K.M., 1988. Microbial methane in the shallow Paleozoic sediments and glacial
506 deposits of Illinois, U.S.A. *Chem. Geol.* 71, 23–40. [https://doi.org/10.1016/0009-2541\(88\)90103-9](https://doi.org/10.1016/0009-2541(88)90103-9)

507 Cornell, R.M., Schwertmann, U., 2003. *The Iron Oxides: Structure, Properties, Reactions, Occurrences and Uses*,
508 second. ed. Wiley-VCH, Weinheim. <https://doi.org/10.1002/3527602097>

509 Cubadda, F., Ciardullo, S., D'Amato, M., Raggi, A., Aureli, F., Carcea, M., 2010. Arsenic Contamination of the
510 Environment–Food Chain: A Survey on Wheat as a Test Plant To Investigate Phytoavailable Arsenic in Italian
511 Agricultural Soils and as a Source of Inorganic Arsenic in the Diet. *J. Agric. Food Chem.* 58, 10176–10183.
512 <https://doi.org/10.1021/jf102084p>

513 Desbarats, A.J., Koenig, C.E.M., Pal, T., Mukherjee, P.K., Beckie, R.D., 2014. Groundwater flow dynamics and arsenic
514 source characterization in an aquifer system of West Bengal, India. *Water Resour. Res.* 50, 4974–5002.
515 <https://doi.org/10.1002/2013WR014034>

516 D. M. S. 14.06.17, 2017. Decreto del Ministero della Salute 14 giugno 2017 sul recepimento della direttiva (UE)
517 2015/1787 che modifica gli allegati II e III della direttiva 98/83/CE sulla qualita' delle acque destinate al
518 consumo umano "Italian Ministerial Decree 14.06.17 on the implementation of Directive 2015/1787/EC
519 amending Annexes II and III to Council Directive 98/83/EC on the quality of water intended for human
520 consumption".

521 Di Giuseppe, D., Bianchini, G., Vittori Antisari, L., Martucci, A., Natali, C., Beccaluva, L., 2014. Geochemical
522 characterization and biomonitoring of reclaimed soils in the Po River Delta (Northern Italy): implications for the
523 agricultural activities. *Environ. Monit. Assess.* 186, 2925–2940. <https://doi.org/10.1007/s10661-013-3590-8>

524 Eberle, A., Besold, J., Kerl, C.F., Lezama-Pacheco, J.S., Fendorf, S., Planer-Friedrich, B., 2020. Arsenic Fate in Peat
525 Controlled by the pH-Dependent Role of Reduced Sulfur. *Environ. Sci. Technol.* 54, 6682–6692.
526 <https://doi.org/10.1021/acs.est.0c00457>

527 EC, 2015. European Commission Directive 2015/1787 of 6 October 2015 amending Annexes II and III to Council
528 Directive 98/83/EC on the quality of water intended for human consumption.

529 Erickson, M.L., Barnes, R.J., 2005. Well characteristics influencing arsenic concentrations in ground water. *Water Res.*
530 39, 4029–4039. <https://doi.org/10.1016/j.watres.2005.07.026>

531 Ersbøll, A.K., Monrad, M., Sørensen, M., Bastrup, R., Hansen, B., Bach, F.W., Tjønneland, A., Overvad, K.,
532 Raaschou-Nielsen, O., 2018. Low-level exposure to arsenic in drinking water and incidence rate of stroke: A
533 cohort study in Denmark. *Environ. Int.* 120, 72–80. <https://doi.org/10.1016/j.envint.2018.07.040>

534 Fendorf, S., Michael, H.A., van Geen, A., 2010. Spatial and Temporal Variations of Groundwater Arsenic in South and
535 Southeast Asia. *Science* 328, 1123–1127. <https://doi.org/10.1126/science.1172974>

536 Fritz, S.J., 1994. A Survey of Charge-Balance Errors on Published Analyses of Potable Ground and Surface Waters.
537 *Groundwater* 32, 539–546. <https://doi.org/10.1111/j.1745-6584.1994.tb00888.x>

538 Gerritse, R.G., George, R.J., 1988. The role of soil organic matter in the geochemical cycling of chloride and bromide.

539 J. Hydrol. 101, 83–95. [https://doi.org/10.1016/0022-1694\(88\)90029-7](https://doi.org/10.1016/0022-1694(88)90029-7)

540 Giuliano, G., 1995. Ground water in the Po basin: some problems relating to its use and protection. *Sci. Total Environ.*

541 171, 17–27. [https://doi.org/10.1016/0048-9697\(95\)04682-1](https://doi.org/10.1016/0048-9697(95)04682-1)

542 Gyuró, É.K., 2007. The Pannonian Great Plain a flourishing garden?: Water as a key to the history and future of the

543 central lowlands in the Carpathian basin. In: Pedroli, B., van Doorn, A., de Blust, G., (Eds.), *Europe's Living*

544 *Landscapes*. KNNV Publishing, Leiden, pp. 294–309. https://doi.org/10.1163/9789004278073_019

545 Hansen, L.K., Jakobsen, R., Postma, D., 2001. Methanogenesis in a shallow sandy aquifer, Rømø, Denmark. *Geochim.*

546 *Cosmochim. Acta* 65, 2925–2935. [https://doi.org/10.1016/S0016-7037\(01\)00653-6](https://doi.org/10.1016/S0016-7037(01)00653-6)

547 Hoehler, T.M., 2004. Biological energy requirements as quantitative boundary conditions for life in the subsurface.

548 *Geobiology* 2, 205–215. <https://doi.org/10.1111/j.1472-4677.2004.00033.x>

549 Hoehler, T.M., Alperin, M.J., Albert, D.B., Martens, C.S., 2001. Apparent minimum free energy requirements for

550 methanogenic Archaea and sulfate-reducing bacteria in an anoxic marine sediment. *FEMS Microbiol. Ecol.* 38,

551 33–41. <https://doi.org/10.1111/j.1574-6941.2001.tb00879.x>

552 Hoehler, T.M., Alperin, M.J., Albert, D.B., Martens, C.S., 1994. Field and Laboratory Studies of Methane Oxidation in

553 an Anoxic Marine Sediment: Evidence for a Methanogen-Sulfate Reducer Consortium. *Global Biogeochem. Cy.*

554 8, 451–463. <https://doi.org/10.1029/94GB01800>

555 Jakobsen, R., 2007. Redox microniches in groundwater: A model study on the geometric and kinetic conditions

556 required for concomitant Fe oxide reduction, sulfate reduction, and methanogenesis. *Water Resour. Res.* 43,

557 W12S12. <https://doi.org/10.1029/2006WR005663>

558 Jakobsen, R., Cold, L., 2007. Geochemistry at the sulfate reduction–methanogenesis transition zone in an anoxic

559 aquifer—A partial equilibrium interpretation using 2D reactive transport modeling. *Geochim. Cosmochim. Acta*

560 71, 1949–1966. <https://doi.org/10.1016/J.GCA.2007.01.013>

561 Jin, Q., Bethke, C.M., 2009. Cellular energy conservation and the rate of microbial sulfate reduction. *Geology* 37,

562 1027–1030. <https://doi.org/10.1130/G30185A.1>

563 Jin, Q., Bethke, C.M., 2003. A New Rate Law Describing Microbial Respiration. *Appl. Environ. Microbiol.* 69, 2340–

564 2348. <https://doi.org/10.1128/AEM.69.4.2340-2348.2003>

565 Kelly, W.R., Holm, T.R., Wilson, S.D., Roadcap, G.S., 2005. Arsenic in Glacial Aquifers: Sources and Geochemical

566 Controls. *Groundwater* 43, 500–510. <https://doi.org/10.1111/j.1745-6584.2005.0058.x>

567 Kirk, M.F., Holm, T.R., Park, J., Jin, Q., Sanford, R.A., Fouke, B.W., Bethke, C.M., 2004. Bacterial sulfate reduction

568 limits natural arsenic contamination in groundwater. *Geology* 32, 953–956. <https://doi.org/10.1130/G20842.1>

569 Kocar, B.D., Benner, S.G., Fendorf, S., 2014. Deciphering and predicting spatial and temporal concentrations of arsenic
570 within the Mekong Delta aquifer. *Environ. Chem.* 11, 579–594. <https://doi.org/10.1071/EN13244>

571 Langner, P., Mikutta, C., Kretzschmar, R., 2012. Arsenic sequestration by organic sulphur in peat. *Nat. Geosci.* 5, 66–
572 73. <https://doi.org/10.1038/ngeo1329>

573 Lindquist, S.J., 1999. Petroleum systems of the Po Basin Province of northern Italy and the northern Adriatic Sea; Porto
574 Garibaldi (biogenic), Meride/Riva di Solto (thermal), and Marnoso Arenacea (thermal). U.S. Geological Survey
575 Open-File Report 99-50-M. <https://doi.org/10.3133/ofr9950M>

576 Lovley, D.R., 1987. Organic matter mineralization with the reduction of ferric iron: A review. *Geomicrobiol. J.* 5, 375–
577 399. <https://doi.org/10.1080/01490458709385975>

578 Lovley, D.R., Goodwin, S., 1988. Hydrogen concentrations as an indicator of the predominant terminal electron-
579 accepting reactions in aquatic sediments. *Geochim. Cosmochim. Acta* 52, 2993–3003.
580 [https://doi.org/10.1016/0016-7037\(88\)90163-9](https://doi.org/10.1016/0016-7037(88)90163-9)

581 Maesano, F.E., D’Ambrogi, C., 2016. Coupling sedimentation and tectonic control: Pleistocene evolution of the central
582 Po Basin. *Ital. J. Geosci.* 135, 394–407. <https://doi.org/10.3301/IJG.2015.17>

583 Marchetti, M., 2002. Environmental changes in the central Po Plain (northern Italy) due to fluvial modifications and
584 anthropogenic activities. *Geomorphology* 44, 361–373. [https://doi.org/10.1016/S0169-555X\(01\)00183-0](https://doi.org/10.1016/S0169-555X(01)00183-0)

585 Martinelli, G., Chahoud, A., Dadomo, A., Fava, A., 2014. Isotopic features of Emilia-Romagna region (North Italy)
586 groundwaters: Environmental and climatological implications. *J. Hydrol.* 519, 1928–1938.
587 <https://doi.org/10.1016/J.JHYDROL.2014.09.077>

588 Mattavelli, L., Novelli, L., 1988. Geochemistry and habitat of natural gases in Italy. *Org. Geochem.* 13, 1–13.
589 [https://doi.org/10.1016/0146-6380\(88\)90021-6](https://doi.org/10.1016/0146-6380(88)90021-6)

590 Mattavelli, L., Ricchiuto, T., Grignani, D., Schoell, M., 1983. Geochemistry and Habitat of Natural Gases in Po Basin,
591 Northern Italy. *Am. Assoc. Pet. Geol. Bull.* 67, 2239–2254.

592 McArthur, J.M., 2019. Arsenic in Groundwater, in: Sikdar, P.K. (Ed.), *Groundwater Development and Management: Issues and Challenges in South Asia*. Springer International Publishing, Cham, pp. 279–308.
593 https://doi.org/10.1007/978-3-319-75115-3_12

594

595 McArthur, J., Banerjee, D., Hudson-Edwards, K., Mishra, R., Purohit, R., Ravenscroft, P., Cronin, A., Howarth, R.,
596 Chatterjee, A., Talukder, T., Lowry, D., Houghton, S., Chadha, D., 2004. Natural organic matter in sedimentary
597 basins and its relation to arsenic in anoxic ground water: the example of West Bengal and its worldwide
598 implications. *Appl. Geochem.* 19, 1255–1293. <https://doi.org/10.1016/J.APGEOCHEM.2004.02.001>

599

- 600 McArthur, J.M., Ravenscroft, P., Banerjee, D.M., Milsom, J., Hudson-Edwards, K.A., Sengupta, S., Bristow, C., Sarkar,
601 A., Tonkin, S., Purohit, R., 2008. How paleosols influence groundwater flow and arsenic pollution: A model from
602 the Bengal Basin and its worldwide implication. *Water Resour. Res.* 44, W11411.
603 <https://doi.org/10.1029/2007WR006552>
- 604 McArthur, J.M., Ghosal, U., Sikdar, P.K., Ball, J.D., 2016. Arsenic in Groundwater: The Deep Late Pleistocene
605 Aquifers of the Western Bengal Basin. *Environ. Sci. Technol.* 50, 3469–3476.
606 <https://doi.org/10.1021/acs.est.5b02477>
- 607 McMahon, P.B., Chapelle, F.H., 1991. Microbial production of organic acids in aquitard sediments and its role in
608 aquifer geochemistry. *Nature* 349, 233–235. <https://doi.org/10.1038/349233a0>
- 609 McMahon, P.B., Chapelle, F.H., 2008. Redox Processes and Water Quality of Selected Principal Aquifer Systems.
610 *Groundwater* 46, 259–271. <https://doi.org/10.1111/j.1745-6584.2007.00385.x>
- 611 Meliker, J.R., Slotnick, M.J., Avruskin, G.A., Haack, S.K., Nriagu, J.O., 2008. Influence of groundwater recharge and
612 well characteristics on dissolved arsenic concentrations in southeastern Michigan groundwater. *Environ.*
613 *Geochem. Health* 31, 147. <https://doi.org/10.1007/s10653-008-9173-x>
- 614 Mihajlov, I., Mozumder, M.R.H., Bostick, B.C., Stute, M., Mailloux, B.J., Knappett, P.S.K., Choudhury, I., Ahmed,
615 K.M., Schlosser, P., van Geen, A., 2020. Arsenic contamination of Bangladesh aquifers exacerbated by clay
616 layers. *Nat. Commun.* 11, 2244. <https://doi.org/10.1038/s41467-020-16104-z>
- 617 Milkov, A. V., Etiope, G., 2018. Revised genetic diagrams for natural gases based on a global dataset of >20,000
618 samples. *Org. Geochem.* 125, 109–120. <https://doi.org/10.1016/j.orggeochem.2018.09.002>
- 619 Miola, A., Bondesan, A., Corain, L., Favaretto, S., Mozzi, P., Piovan, S., Sostizzo, I., 2006. Wetlands in the Venetian
620 Po Plain (northeastern Italy) during the Last Glacial Maximum: Interplay between vegetation, hydrology and
621 sedimentary environment. *Rev. Palaeobot. Palynol.* 141, 53–81.
622 <https://doi.org/10.1016/J.REVPALBO.2006.03.016>
- 623 Molinari, A., Ayora, C., Marcaccio, M., Guadagnini, L., Sanchez-Vila, X., Guadagnini, A., 2014. Geochemical
624 modeling of arsenic release from a deep natural solid matrix under alternated redox conditions. *Environ. Sci.*
625 *Pollut. Res.* 21, 1628–1637. <https://doi.org/10.1007/s11356-013-2054-6>
- 626 Molinari, A., Guadagnini, L., Marcaccio, M., Guadagnini, A., 2015. Arsenic fractioning in natural solid matrices
627 sampled in a deep groundwater body. *Geoderma* 247–248, 88–96.
628 <https://doi.org/10.1016/j.geoderma.2015.02.011>

- 629 Molinari, A., Guadagnini, L., Marcaccio, M., Straface, S., Sanchez-Vila, X., Guadagnini, A., 2013. Arsenic release
630 from deep natural solid matrices under experimentally controlled redox conditions. *Sci. Total Environ.* 444, 231–
631 240. <https://doi.org/10.1016/J.SCITOTENV.2012.11.093>
- 632 Murphy, E.M., Schramke, J.A., Fredrickson, J.K., Bledsoe, H.W., Francis, A.J., Sklarew, D.S., Linehan, J.C., 1992. The
633 influence of microbial activity and sedimentary organic carbon on the isotope geochemistry of the Middendorf
634 Aquifer. *Water Resour. Res.* 28, 723–740. <https://doi.org/10.1029/91WR02678>
- 635 Nickson, R., McArthur, J., Burgess, W., Ahmed, K.M., Ravenscroft, P., Rahman, M., 1998. Arsenic poisoning of
636 Bangladesh groundwater. *Nature* 395, 338. <https://doi.org/10.1038/26387>
- 637 O'Day, P.A., Vlassopoulos, D., Root, R., Rivera, N., 2004. The influence of sulfur and iron on dissolved arsenic
638 concentrations in the shallow subsurface under changing redox conditions. *Proc. Natl. Acad. Sci. U. S. A.* 101,
639 13703–13708. <https://doi.org/10.1073/pnas.0402775101>
- 640 Ori, G.G., 1993. Continental depositional systems of the Quaternary of the Po Plain (northern Italy). *Sediment. Geol.*
641 83, 1–14. [https://doi.org/10.1016/S0037-0738\(10\)80001-6](https://doi.org/10.1016/S0037-0738(10)80001-6)
- 642 Parkhurst, D.L., Appelo, C.A.J., 2013. Description of input and examples for PHREEQC version 3: A computer
643 program for speciation, batch-reaction, one-dimensional transport, and inverse geochemical calculations. U. S.
644 Geological Survey Techniques and Methods 6-A4, Book 6, Chapter 43.
- 645 Perego, R., Bonomi, T., Fumagalli, M.L., Benastini, V., Aghib, F., Rotiroti, M., Cavallin, A., 2014. 3D reconstruction
646 of the multi-layer aquifer in a Po Plain area. *Rend. Online Soc. Geol. Ital.* 30, 41–44.
647 <https://doi.org/10.3301/ROL.2014.09>
- 648 Planer-Friedrich, B., Härtig, C., Lissner, H., Steinborn, J., Süß, E., Qumrul Hassan, M., Zahid, A., Alam, M., Merkel,
649 B., 2012. Organic carbon mobilization in a Bangladesh aquifer explained by seasonal monsoon-driven storativity
650 changes. *Appl. Geochem.* 27, 2324–2334. <https://doi.org/10.1016/j.apgeochem.2012.08.005>
- 651 Postma, D., 1982. Pyrite and siderite formation in brackish and freshwater swamp sediments. *Am. J. Sci.* 282, 1151–
652 1183. <https://doi.org/10.2475/ajs.282.8.1151>
- 653 Postma, D., Jakobsen, R., 1996. Redox zonation: Equilibrium constraints on the Fe(III)/SO₄-reduction interface.
654 *Geochim. Cosmochim. Acta* 60, 3169–3175. [https://doi.org/10.1016/0016-7037\(96\)00156-1](https://doi.org/10.1016/0016-7037(96)00156-1)
- 655 Postma, D., Larsen, F., Minh Hue, N.T., Duc, M.T., Viet, P.H., Nhan, P.Q., Jessen, S., 2007. Arsenic in groundwater of
656 the Red River floodplain, Vietnam: Controlling geochemical processes and reactive transport modeling. *Geochim.*
657 *Cosmochim. Acta* 71, 5054–5071. <https://doi.org/10.1016/J.GCA.2007.08.020>
- 658 Postma, D., Larsen, F., Thai, N.T., Trang, P.T.K., Jakobsen, R., Nhan, P.Q., Long, T.V., Viet, P.H., Murray, A.S., 2012.

659 Groundwater arsenic concentrations in Vietnam controlled by sediment age. *Nat. Geosci.* 5, 656–661.
660 <https://doi.org/10.1038/ngeo1540>

661 Radloff, K.A., Zheng, Y., Stute, M., Weinman, B., Bostick, B., Mihajlov, I., Bounds, M., Rahman, M.M., Huq, M.R.,
662 Ahmed, K.M., Schlosser, P., van Geen, A., 2017. Reversible adsorption and flushing of arsenic in a shallow,
663 Holocene aquifer of Bangladesh. *Appl. Geochem.* 77, 142–157. <https://doi.org/10.1016/j.apgeochem.2015.11.003>

664 Ravenscroft, P., Brammer, H., Richards, K., 2009. *Arsenic Pollution: A Global Synthesis*. Wiley-Blackwell, Chichester.
665 <https://doi.org/10.1002/9781444308785>

666 Ravenscroft, P., McArthur, J.M., Hoque, B.A., 2001. Geochemical and Palaeohydrological Controls on Pollution of
667 Groundwater by Arsenic., in: Chappell, W.R., Abernathy, C.O., Calderon, R.L. (Eds.), *Arsenic Exposure and*
668 *Health Effects IV*. Elsevier Science Ltd, Oxford, pp. 53–78.

669 Richards, L.A., Magnone, D., Sültenfuß, J., Chambers, L., Bryant, C., Boyce, A.J., van Dongen, B.E., Ballentine, C.J.,
670 Sovann, C., Uhlemann, S., Kuras, O., Goody, D.C., Polya, D.A., 2019. Dual in-aquifer and near surface
671 processes drive arsenic mobilization in Cambodian groundwaters. *Sci. Total Environ.* 659, 699–714.
672 <https://doi.org/10.1016/j.scitotenv.2018.12.437>

673 Rossi, M., Minervini, M., Ghielmi, M., Rogledi, S., 2015. Messinian and Pliocene erosional surfaces in the Po Plain-
674 Adriatic Basin: Insights from allostratigraphy and sequence stratigraphy in assessing play concepts related to
675 accommodation and gateway turnarounds in tectonically active margins. *Mar. Pet. Geol.* 66, 192–216.
676 <https://doi.org/10.1016/j.marpetgeo.2014.12.012>

677 Rotiroti, M., Bonomi, T., Sacchi, E., McArthur, J.M., Stefania, G.A., Zanotti, C., Taviani, S., Patelli, M., Nava, V.,
678 Soler, V., Fumagalli, L., Leoni, B., 2019a. The effects of irrigation on groundwater quality and quantity in a
679 human-modified hydro-system: The Oglio River basin, Po Plain, northern Italy. *Sci. Total Environ.* 672, 342–356.
680 <https://doi.org/10.1016/J.SCITOTENV.2019.03.427>

681 Rotiroti, M., Jakobsen, R., Fumagalli, L., Bonomi, T., 2018. Considering a threshold energy in reactive transport
682 modeling of microbially mediated redox reactions in an arsenic-affected aquifer. *Water* 10, 90.
683 <https://doi.org/10.3390/w10010090>

684 Rotiroti, M., Jakobsen, R., Fumagalli, L., Bonomi, T., 2015. Arsenic release and attenuation in a multilayer aquifer in
685 the Po Plain (northern Italy): Reactive transport modeling. *Appl. Geochem.* 63, 599–609.
686 <https://doi.org/10.1016/j.apgeochem.2015.07.001>

687 Rotiroti, M., McArthur, J., Fumagalli, L., Stefania, G.A., Sacchi, E., Bonomi, T., 2017. Pollutant sources in an arsenic-
688 affected multilayer aquifer in the Po Plain of Italy: Implications for drinking-water supply. *Sci. Total Environ.*

689 578, 502–512. <https://doi.org/10.1016/j.scitotenv.2016.10.215>

690 Rotiroti, M., Sacchi, E., Fumagalli, L., Bonomi, T., 2014. Origin of arsenic in groundwater from the multilayer aquifer
691 in cremona (Northern Italy). *Environ. Sci. Technol.* 48, 5395–5403. <https://doi.org/10.1021/es405805v>

692 Rotiroti, M., Zanotti, C., Fumagalli, L., Taviani, S., Stefania, G.A., Patelli, M., Nava, V., Soler, V., Sacchi, E., Leoni,
693 B., 2019b. Multivariate statistical analysis supporting the hydrochemical characterization of groundwater and
694 surface water: A case study in northern Italy. *Rend. Online Soc. Geol. Ital.* 47, 90–96.
695 <https://doi.org/10.3301/ROL.2019.17>

696 Rowland, H.A.L., Omoregie, E.O., Millot, R., Jimenez, C., Mertens, J., Baciu, C., Hug, S.J., Berg, M., 2011.
697 Geochemistry and arsenic behaviour in groundwater resources of the Pannonian Basin (Hungary and Romania).
698 *Appl. Geochem.* 26, 1–17. <https://doi.org/10.1016/J.APGEOCHEM.2010.10.006>

699 Sciarra, A., Cinti, D., Pizzino, L., Procesi, M., Voltattorni, N., Mecozzi, S., Quattrocchi, F., 2013. Geochemistry of
700 shallow aquifers and soil gas surveys in a feasibility study at the Rivara natural gas storage site (Po Plain,
701 Northern Italy). *Appl. Geochem.* 34, 3–22. <https://doi.org/10.1016/J.APGEOCHEM.2012.11.008>

702 Sø, H.U., Postma, D., Vi, M.L., Pham, T.K.T., Kazmierczak, J., Dao, V.N., Pi, K., Koch, C.B., Pham, H.V., Jakobsen,
703 R., 2018. Arsenic in Holocene aquifers of the Red River floodplain, Vietnam: Effects of sediment-water
704 interactions, sediment burial age and groundwater residence time. *Geochim. Cosmochim. Acta* 225, 192–209.
705 <https://doi.org/10.1016/J.GCA.2018.01.010>

706 Sracek, O., Berg, M., Müller, B., 2018. Redox buffering and de-coupling of arsenic and iron in reducing aquifers across
707 the Red River Delta, Vietnam, and conceptual model of de-coupling processes. *Environ. Sci. Pollut. Res.* 25,
708 15954–15961. <https://doi.org/10.1007/s11356-018-1801-0>

709 Stuckey, J.W., Schaefer, M.V., Kocar, B.D., Benner, S.G., Fendorf, S., 2016. Arsenic release metabolically limited to
710 permanently water-saturated soil in Mekong Delta. *Nat. Geosci.* 9, 70–76. <https://doi.org/10.1038/ngeo2589>

711 Sutton, N.B., van der Kraan, G.M., van Loosdrecht, M.C.M., Muyzer, G., Bruining, J., Schotting, R.J., 2009.
712 Characterization of geochemical constituents and bacterial populations associated with As mobilization in deep
713 and shallow tube wells in Bangladesh. *Water Res.* 43, 1720–1730.
714 <https://doi.org/10.1016/J.WATRES.2009.01.006>

715 Wang, Y.H., Li, P., Dai, X.Y., Zhang, R., Jiang, Z., Jiang, D.W., Wang, Y.X., 2015. Abundance and diversity of
716 methanogens: Potential role in high arsenic groundwater in Hetao Plain of Inner Mongolia, China. *Sci. Total*
717 *Environ.* 515–516, 153–161. <https://doi.org/10.1016/J.SCITOTENV.2015.01.031>

718 Welch, A.H., Westjohn, D.B., Helsel, D.R., Wanty, R.B., 2000. Arsenic in Ground Water of the United States:

719 Occurrence and Geochemistry. *Groundwater* 38, 589–604. <https://doi.org/10.1111/j.1745-6584.2000.tb00251.x>

720 Whiticar, M.J., 1999. Carbon and hydrogen isotope systematics of bacterial formation and oxidation of methane. *Chem.*

721 *Geol.* 161, 291–314. [https://doi.org/10.1016/S0009-2541\(99\)00092-3](https://doi.org/10.1016/S0009-2541(99)00092-3)

722 WHO, 2011. Guidelines for drinking-water quality, 4th edition. World Health Organization, Geneva.

723 Winkel, L.H.E., Trang, P.T.K., Lan, V.M., Stengel, C., Amini, M., Ha, N.T., Viet, P.H., Berg, M., 2011. Arsenic

724 pollution of groundwater in Vietnam exacerbated by deep aquifer exploitation for more than a century. *Proc. Natl.*

725 *Acad. Sci. U. S. A.* 108, 1246–1251. <https://doi.org/10.1073/pnas.1011915108>

726 Yao, H., Conrad, R., 1999. Thermodynamics of Methane Production in Different Rice Paddy Soils from China, the

727 Philippines and Italy. *Soil Biol. Biochem.* 31, 463–473; [https://doi.org/10.1016/S0038-0717\(98\)00152-7](https://doi.org/10.1016/S0038-0717(98)00152-7)

728 Zanotti, C., Rotiroti, M., Fumagalli, L., Stefania, G.A., Canonaco, F., Stefanelli, G., Prévôt, A.S.H., Leoni, B., Bonomi,

729 T., 2019. Groundwater and surface water quality characterization through positive matrix factorization combined

730 with GIS approach. *Water Res.* 159, 122–134. <https://doi.org/10.1016/j.watres.2019.04.058>

731 Zhou, S., Xu, J., Yang, G., Zhuang, L., 2014. Methanogenesis affected by the co-occurrence of iron(III) oxides and

732 humic substances. *FEMS Microbiol. Ecol.* 88, 107–120. <https://doi.org/10.1111/1574-6941.12274>

733 Zuppi, G.M., Sacchi, E., 2004. Hydrogeology as a climate recorder: Sahara–Sahel (North Africa) and the Po Plain

734 (Northern Italy). *Glob. Planet. Change* 40, 79–91. [https://doi.org/10.1016/S0921-8181\(03\)00099-7](https://doi.org/10.1016/S0921-8181(03)00099-7)

735 Zuzolo, D., Cicchella, D., Demetriades, A., Birke, M., Albanese, S., Dinelli, E., Lima, A., Valera, P., De Vivo, B.,

736 2020. Arsenic: Geochemical distribution and age-related health risk in Italy. *Environ. Res.* 182, 109076.

737 <https://doi.org/10.1016/J.ENVRES.2019.109076>

738

739

740 **Figure Captions**

741

742 Fig. 1. Scatter plots of DOC vs NH_4 , total phosphorus (P-tot), Cl/Br, CH_4 , alkalinity, and EC. Fered-SO₄redEARL:
743 groundwaters under Fe-oxide reduction and early-stage sulfate reduction; Fered-SO₄redADV: groundwaters under Fe-
744 oxide reduction and advanced-stage sulfate reduction; Fered-CH₄gen: groundwaters under Fe-oxide reduction and
745 methanogenesis.

746

747 Fig. 2. Testing the “partial” equilibrium state in the studied system. a) Equilibrium diagram of the simultaneous
748 equilibrium of Fe-oxide reduction, sulfate reduction and FeS precipitation (black lines), and Fe-oxide reduction and
749 methanogenesis (orange line) for different Fe-oxides; see Table S4 for reactions and equilibrium line equations. The
750 equilibrium lines are plotted considering a value of -3 for $\log[\text{SO}_4^{2-}]$, according to Postma and Jakobsen (1996), and
751 average measured values of -2.35 for $\log[\text{HCO}_3^-]$ and -6.21 for $\log[\text{CH}_4]$. b) Computed available energy at system
752 conditions (symbols) over threshold energy (dotted lines) for Fe-oxide reduction, sulfate reduction and methanogenesis;
753 threshold energy values are from (a) Rotiroti et al., 2018 (b) Jakobsen and Cold, 2007 (c) Hoehler et al., 2001 (d)
754 Hoehler et al., 1994 (e) Yao and Conrad, 1999. Fered-SO₄redEARL: groundwaters under Fe-oxide reduction and early-
755 stage sulfate reduction; Fered-SO₄redADV: groundwaters under Fe-oxide reduction and advanced-stage sulfate
756 reduction; Fered-CH₄gen: groundwaters under Fe-oxide reduction and methanogenesis.

757

758 Fig. 3. Scatter plots of As vs DOC, total phosphorus (P-tot), Cl/Br, Fe, SO_4 and CH_4 . Fered-SO₄redEARL:
759 groundwaters under Fe-oxide reduction and early-stage sulfate reduction; Fered-SO₄redADV: groundwaters under Fe-
760 oxide reduction and advanced-stage sulfate reduction; Fered-CH₄gen: groundwaters under Fe-oxide reduction and
761 methanogenesis.

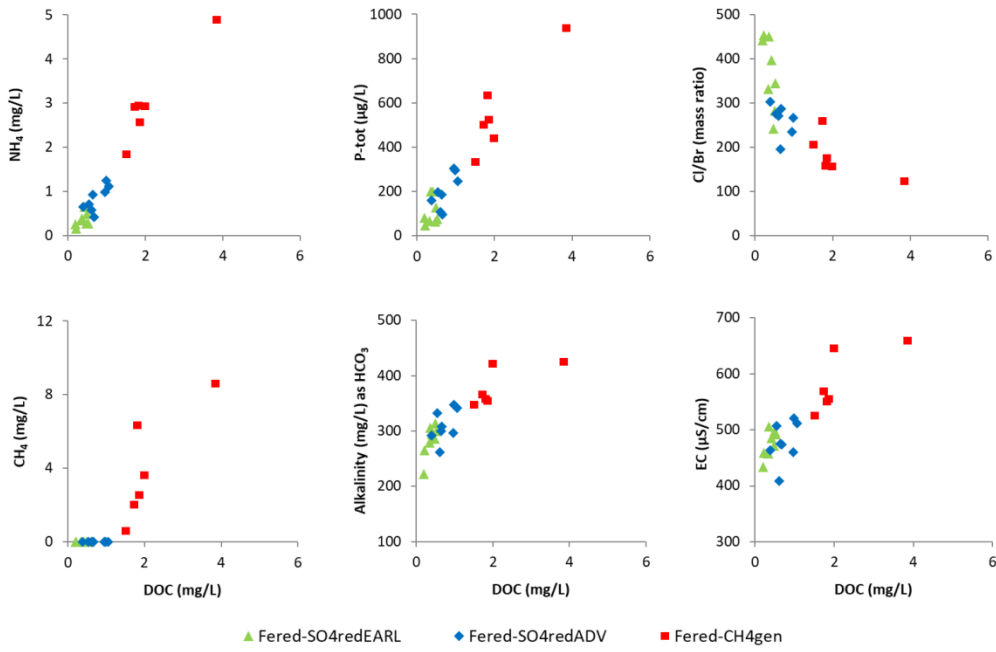
762

763 Fig. 4. Schematization of the evolution of the concentration of As and the main redox-sensitive species, together with
764 related main processes, with the progression of peat degradation; see the text for a detailed explanation. For the bar
765 “Sampled groundwater in this study”, the green part refers to samples classified under Fe-oxide reduction and early-
766 stage sulfate reduction, the blue refers to Fe-oxide reduction and advanced-stage sulfate reduction, and the red to Fe-
767 oxide reduction and methanogenesis.

768

769

770 Fig. 1.



771

772

773

774

775

776

777

778

779

780

781

782

783

784

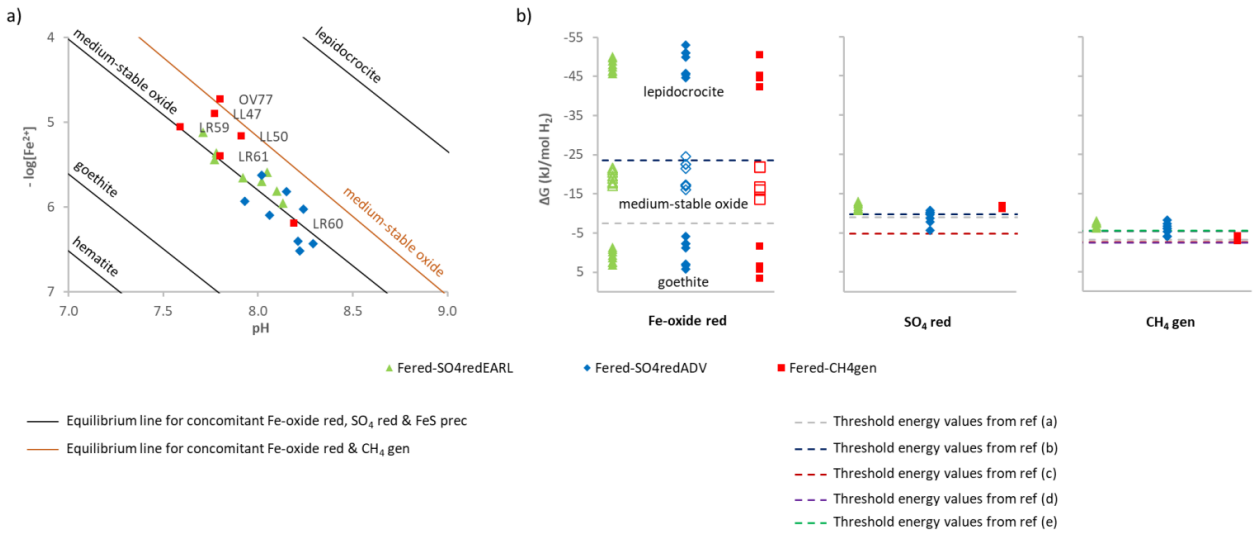
785

786

787

788

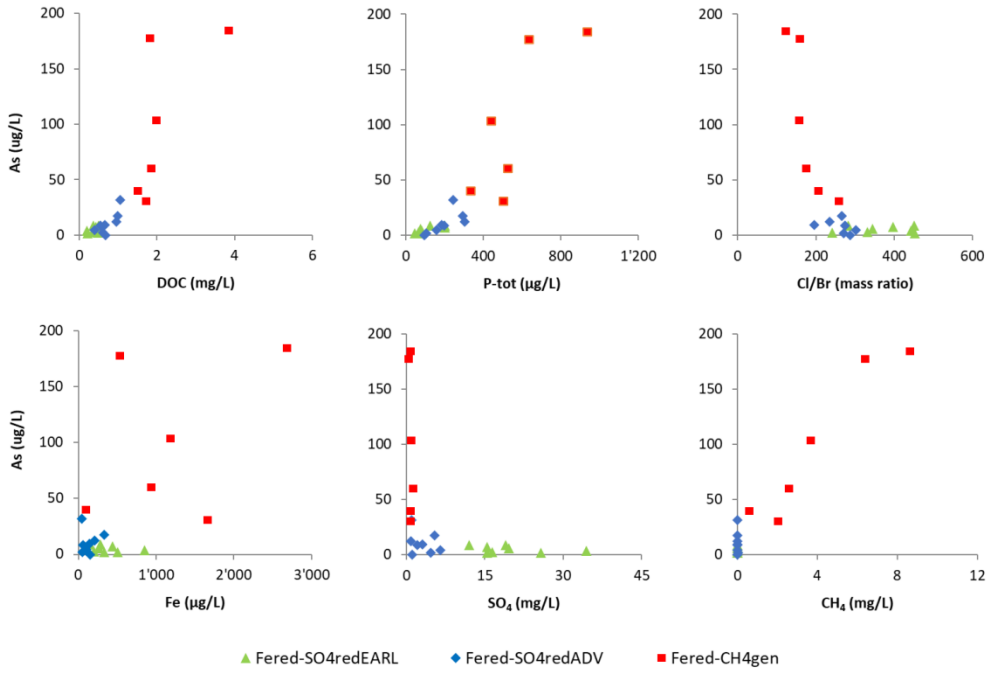
789 Fig. 2



790
 791
 792
 793
 794
 795
 796
 797
 798
 799
 800
 801
 802
 803
 804
 805
 806
 807
 808
 809
 810
 811

812 Fig 3

813



814

815

816

817

818

819

820

821

822

823

824

825

826

827

828

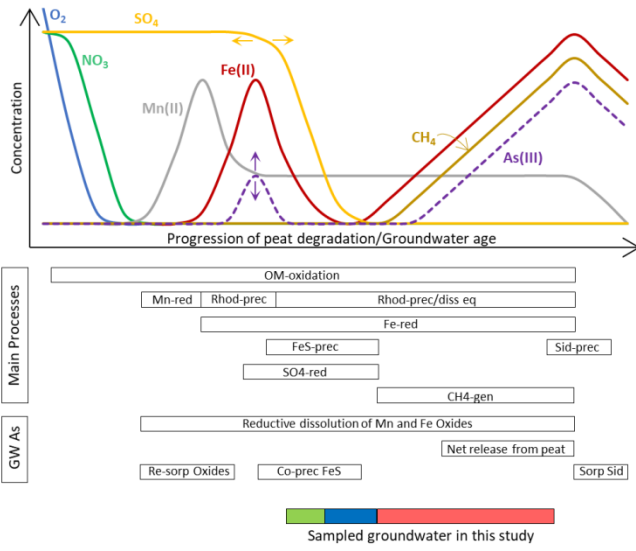
829

830

831

832 Fig. 4.

833



834